PERGAMON

Journal of Structural Geology 24 (2002) 1451–1462

JOURNAL OF STRUCTURAL GEOLOGY

www.elsevier.com/locate/jstrugeo

Coaxial flattening at deep levels of orogenic belts: evidence from blueschists and eclogites on Syros and Sifnos (Cyclades, Greece)

Gideon Rosenbaum*, Dov Avigad, Mario Sánchez-Gómez[1]

Institute of Earth Sciences, Hebrew University of Jerusalem, Jerusalem 91904, Israel

Received 9 May 2001; revised 17 October 2001; accepted 24 October 2001

Abstract

This work presents new structural data from a high-pressure/low-temperature (HP/LT) metamorphic terrane exposed on the islands of Syros and Sifnos (Cyclades, Greece). The structure and the metamorphism of a relatively coherent HP/LT rock section were studied in order to elucidate how strain was accommodated at deep crustal levels during the formation and exhumation of HP/LT rocks. At least three deformation phases associated with eclogite- and blueschist-facies conditions ($P = 8$–15 kbar; $T = 400$–550 °C) were recognised. The earliest deformation fabric (S1), preserved as inclusion trails within garnet porphyroblasts, is aligned to define a sub-vertical schistosity (at present orientation), which is frequently orthogonal to the flat matrix schistosity (S2), and may indicate that deep crustal thickening involved upright folding. The currently dominant fabric in the HP rock section, S2, is usually moderately dipping and locally contains NW-trending glaucophane lineations, symmetric pressure-shadows and eclogitic boudins. The symmetric structures associated with this fabric seem to indicate coaxial vertical thinning, although the existence of non-coaxial structures out of the study area cannot be excluded. Glaucophane-bearing shear bands (S3), with top-to-NW sense of shearing, locally crosscut the earlier structures. The latest recognised fabric (D4) is scarce and often absent within the HP rocks. It is associated with top-to-NE kinematic criteria that formed at greenschist-facies conditions ($P = 4$–7 kbar; $T = 400$–450 °C). Based on these observations, it is suggested that partitioning of strain occurred at different crustal levels and at different times. Deep crustal deformation was governed by thickening via upright folding followed by coaxial vertical thinning, whereas non-coaxial shearing occurred when the rocks were already exhumed to relatively shallow crustal levels. The earliest fabrics (D1 to D3) pertain to Alpine orogenesis and possibly to syn-orogenic extension, whereas the latest correspond to whole-crust back-arc extension.

Keywords: Cyclades; Exhumation; Extension; Sifnos; Syros

1. Introduction

Exhumation processes of high-pressure/low-temperature (HP/LT) rocks have been extensively discussed in the geological literature (see review papers by Platt (1993) and Ring et al. (1999)). HP rocks are usually exposed in orogenic belts, and their exhumation has been commonly attributed to syn-orogenic or post-orogenic extension (Platt, 1986; Dewey, 1988; Avigad et al., 1997; Jolivet et al., 1998). Typical structures found in extensional orogenic domains are metamorphic core complexes. These structures accommodated horizontal extension by movement along flat-lying shear zones and low-angle normal-sense detachment faults, and they are marked by asymmetric kinematic criteria indicative of non-coaxial shearing (e.g. Lister and Davis, 1989). The recognition of metamorphic core complexes in various orogenic belts has provided a plausible mechanism for the exhumation and the preservation of HP terranes. Examples are: the Norwegian Caledonides (Andersen and Jamtveit, 1990), the Aegean Sea (Lister et al., 1984; Avigad and Garfunkel, 1991; Gautier et al., 1993), Alpine Corsica (Jolivet et al., 1990) and the Alboran Domain (Balanyá et al., 1997; Azañón et al., 1998).

It is important to note, however, that most structures associated with the exhumation of the HP terranes are actually found in greenschist-facies mylonitic shear zones (e.g. Lister et al., 1984; Jolivet et al., 1990). This deformation did not take place at HP conditions. It occurred at relatively shallow crustal levels simultaneously with the dynamic recrystallisation of greenschist-facies assemblages. The aim of this paper is to study how strain was accommodated at deeper crustal levels during the burial and the exhumation of HP terranes.

Deep crustal deformation associated with the exhumation

* Corresponding author. Present address: School of Geosciences, Australian Crustal Research Centre, Monash University, Victoria 3800, Australia. Tel.: +61-3-9905-1532; fax: +61-3-9905-5062.

E-mail address: gideon@mail.earth.monash.edu.au (G. Rosenbaum).

[1] Present address: Departamento de Geología, Unversidad de Jaén, Jaén 23071, Spain.

0191-8141/02/$ - see front matter
PII: S0191-8141(01)00143-2

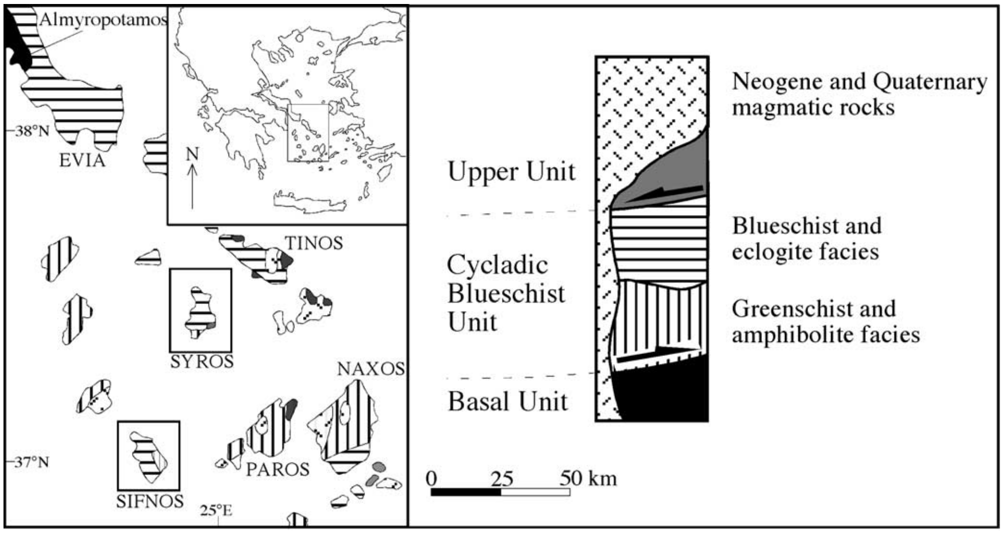

Fig. 1. Simplified geological map of the Cycladic islands and southern Evia modified after Altherr et al. (1979). Boxes indicate the locations of study areas.

of a HP terrane has been studied in the Norwegian Caledonides by Andersen and Jamtveit (1990) and Andersen et al. (1994). These authors have recognised a heterogeneous distribution of extensional deformation in different levels of the crust. In their model, shearing along extensional detachments that occurred in relatively shallow crustal levels was coeval with coaxial strain and pure-shear deformation at deeper levels.

In this paper, we present structural observations from a kilometre-thick coherent HP section, which crops out on the island of Syros and Sifnos in the Cycladic massif (the Aegean Sea) (Fig. 1). During orogenesis, these rocks were buried to high-pressure metamorphic conditions and were subsequently uplifted to upper crustal levels. Structural evidence from the Cycladic massif clearly indicates that non-coaxial strain in the upper crust played a major role during extensional deformation (Lister et al., 1984; Buick, 1991; Faure et al., 1991; Lee and Lister, 1992; Gautier et al., 1993; Gautier and Brun, 1994; Jolivet and Patriat, 1999). We define the style of strain in deeper crustal levels, which formed the root of the orogenic pile. We show that many of these structures are discontinuous with shallower (greenschist-facies) structures, and we note that the style of deformation at HP conditions differs significantly from the typical non-coaxial structures recognised at shallower crustal levels. The dominant fabric identified here (associated with the HP rocks) was probably subjected to coaxial strain and pure-shear vertical thinning.

2. Geological setting

2.1. Structural setting and metamorphism

Rocks in the Cycladic islands and in southern Evia are usually divided into three tectonic units, which are, from bottom to top, the Basal Unit, the Cycladic Blueschist Unit and the Upper Unit (Dürr et al., 1978; Bonneau, 1984) (Fig. 1). The lowermost Basal Unit consists of Mesozoic and Early Cenozoic platform carbonates found in several tectonic windows (Katsikatsos et al., 1986; Avigad and Garfunkel, 1989; Shaked et al., 2000). The Basal Unit is a weakly metamorphosed parautochthonous unit underthrust below the high-pressure rocks of the Cycladic Blueschist Unit. High-pressure relics have recently been found in the Almyropotamos tectonic window (Shaked et al., 2000) (Fig. 1); however, significantly higher metamorphic conditions occurred in the overlying Blueschist Unit. Based on the inverted metamorphic grade sequence, the contact between the Basal Unit and the overlying Blueschist Unit has been classically termed as a major thrust fault that operated sometimes after the Late Eocene (Avigad and Garfunkel, 1989; Shaked et al., 2000).

The Cycladic Blueschist Unit, which occupies an intermediate position within the nappe pile, is the main unit in the Cycladic massif. It consists of meta-sediments and metavolcanics that underwent high-pressure metamorphism (M1) at peak metamorphic conditions of 15 kbar and 500 °C (Dixon, 1976; Matthews and Schliestedt, 1984; Schliestedt, 1986; Okrusch and Bröcker, 1990; Bröcker et al., 1993). In earlier studies, the age of the culmination of HP metamorphism was interpreted as Mid-Eocene (53–40 Ma) (Altherr et al., 1979; Andriessen et al., 1979; Maluski et al., 1987), but it has been suggested that these ages indicate cooling of an earlier metamorphic event (Wijbrans and McDougall, 1988). In recent studies, additional older (60–80 Ma) and younger (32–36 Ma) metamorphic ages have been obtained by geochronological methods (Lister and Raouzaios, 1996; Bröcker and Enders, 1999), and the occurrence of several different metamorphic events was recognised (Forster and Lister, 1999b; Lister

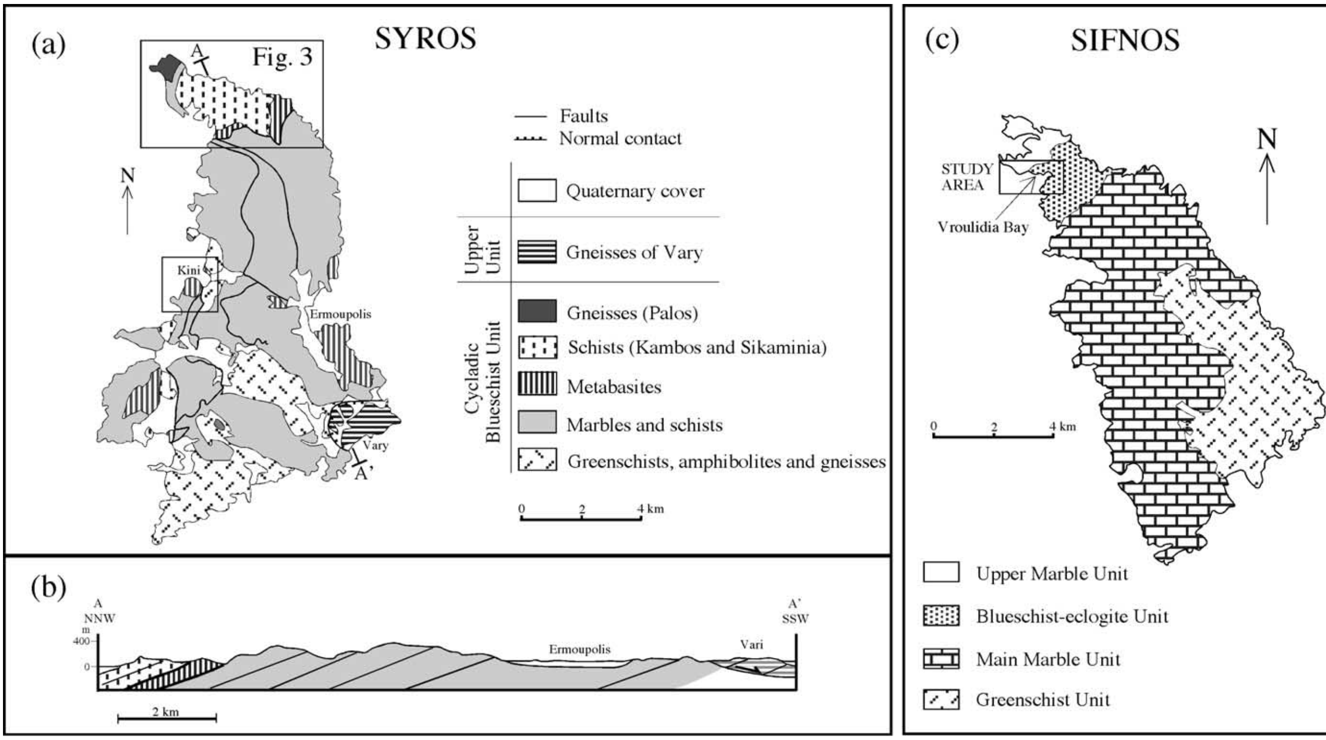

Fig. 2. (a) Geological map of Syros simplified after Hecht (1984) showing the distribution of metabasites within a thick marble-schist sequence. Boxes indicate the location of study areas. (b) Schematic cross-section in Syros (along line A–A′). (c) Simplified geological map of Sifnos (after Davis (1966) and Matthews and Schliestedt (1984)).

et al., 2001). The Cycladic eclogites were probably formed during the latest Cretaceous or the Early Tertiary (Keay, 1998; Bröcker and Enders, 1999), earlier than previously suggested. In most areas, the high-pressure rocks of the Cycladic Blueschist Unit were overprinted by a medium-pressure retrograde metamorphism (M2) 25–20 Ma ago (Altherr et al., 1982; Bröcker et al., 1993), but on the islands of Syros, Sifnos and Tinos, thick eclogite- and blueschist sequences remained intact (Fig. 1).

The top of the Cycladic Blueschist Unit is delimited by low-angle detachment faults recognised on several islands (Avigad and Garfunkel, 1991). These faults separate the Blueschist Unit in the footwall from the unmetamorphosed rocks and low-pressure metamorphic rocks of the Upper Unit (Dürr et al., 1978). Greenschist-facies kinematic markers are widespread below the detachment and usually indicate top-to-NE or top-to-N sense of shear (Urai et al., 1990; Buick, 1991; Faure et al., 1991; Gautier et al., 1993; Gautier and Brun, 1994; Jolivet and Patriat, 1999).

The latest deformation in the Cycladic massif has been predominantly governed by back-arc extension associated with the opening of the Aegean Sea (Le Pichon and Angelier, 1979; Lister et al., 1984; Gautier and Brun, 1994; Avigad et al., 1998). Extension was accompanied or possibly alternated with shortening perpendicular to the stretching direction recognised in large-scale NE–SW to NNE–SSW trending folds (Avigad et al., 2001).

2.2. The geology of Syros

The island of Syros, in the northeastern part of the Cycladic archipelago (Fig. 1), consists of a thick structural succession of the Cycladic Blueschist Unit, and a tectonic slice of the Upper Unit (Fig. 2a and b) (Hecht, 1984; Maluski et al., 1987). Rocks of the Cycladic Blueschist Unit dip N to NE and occupy almost the entire island. They consist of a metasedimentary marble-schist sequence, overthrust by diverse glaucophane-bearing rocks, eclogites, metagabbros, ultramafic rocks and jadeite gneisses (Bonneau et al., 1980a,b; Hecht, 1984). Within the marble-schist sequence, marbles are predominantly calcitic with minor intercalations of dolomites (Bonneau et al., 1980a). The schists, which are considered to represent metamorphosed flysch sediments (Dixon and Ridley, 1987), are metapelitic and metapsammitic with minor intercalations of calcite- and dolomite-bearing schists. Metabasites and ultramafic rocks crop out in various locations throughout the island. These are particularly well preserved south of the village of Kini and in the northern part of the island (Fig. 2a). In the latter, eclogites, metagabbros, glaucophane-schists and serpentinites form a narrow belt, which is tectonically juxtaposed on top of the marble-schist sequence (Fig. 3a). It has been suggested that the origin of this rock association is an ophiolitic mélange or a metamorphosed olistostrome (Bonneau et al., 1980a,b; Dixon and Ridley, 1987). In

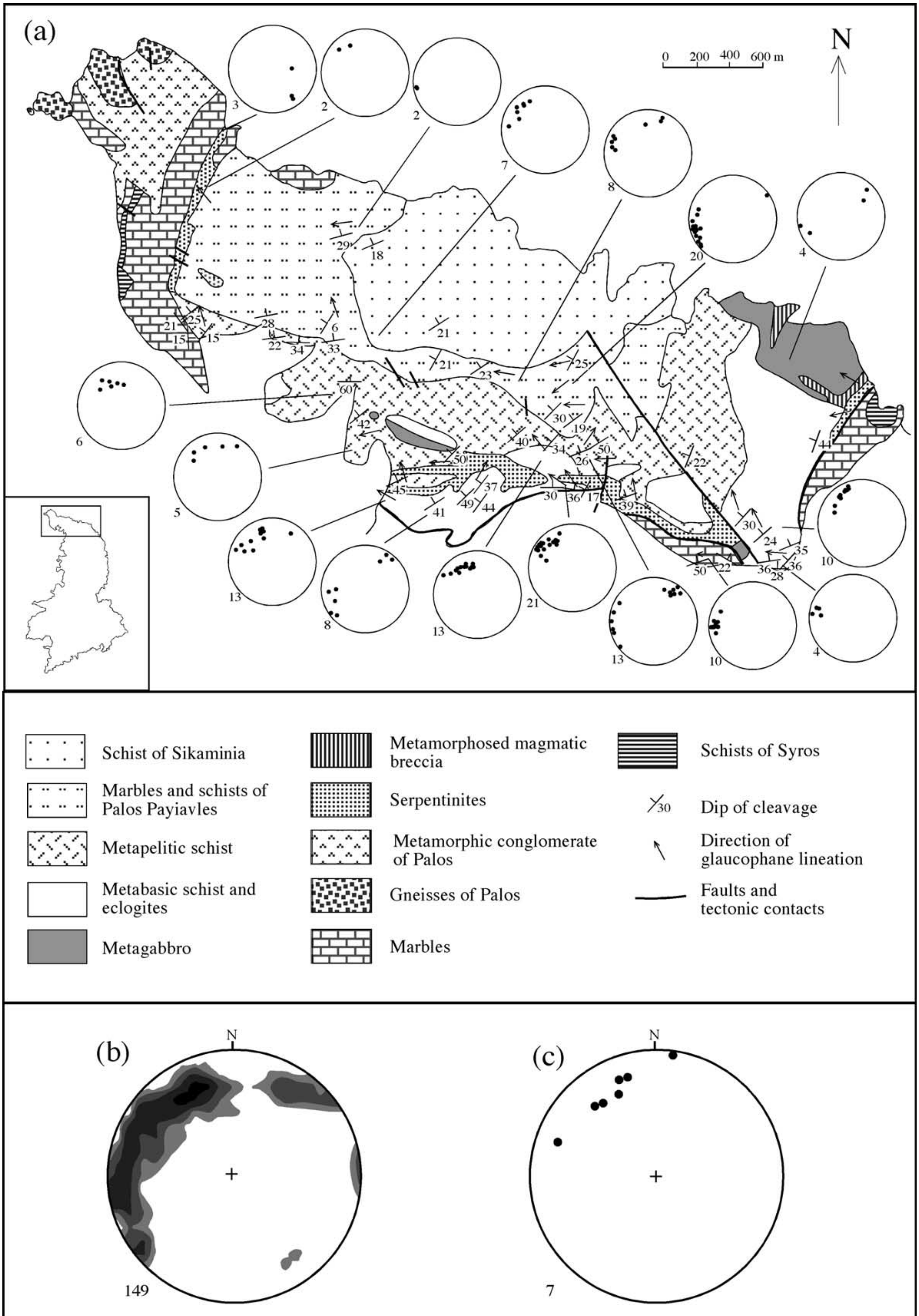

Fig. 3. (a) Geological and structural map of northern Syros (partly modified from Hecht, 1984). Equal area (lower hemisphere) stereograms indicate orientations of glaucophane lineations. (b) Glaucophane lineations in northern Syros plotted on an equal area density stereogram (contours of 1, 2, 4 and 8%). (c) Equal area (lower hemisphere) stereogram showing axes of meso-scale F2 folds within the HP section.

northern Syros, the metabasites are conformably overlain by metapelitic schists, metapsammitic gneisses and marbles (Hecht, 1984) (Fig. 3a).

The occurrence of M2 retrograde metamorphism is rather limited on the island of Syros. In the central and northern parts of the island, the Cycladic Blueschist Unit was occasionally overprinted by greenschist-facies assemblages, whereas in southern Syros, the greenschist-facies overprint was nearly pervasive. However, much of the section in northern Syros is an intact HP sequence, which provides an excellent and unique opportunity to study the style of strain at depth.

The Upper Unit on Syros, which is tectonically above the blueschists and eclogites, consists of a quartzo-feldspatic orthogneiss with no evidence of high-pressure metamorphism (the Vary Gneiss; Fig. 2a and b). Radiometric dating ($^{40}Ar/^{39}Ar$ on phengite) yielded Upper Cretaceous ages (Bonneau et al., 1980a; Maluski et al., 1987), similar to ages obtained on other parts of the Upper Unit throughout the Cyclades (Altherr et al., 1994; Bröcker and Franz, 1998). Avigad and Garfunkel (1989) and Trotet et al. (2001) have interpreted the contact between the Vary Unit and the underlying Blueschist Unit as an extensional fault.

3. Strain geometry on Syros

Observations from major outcrops of eclogite- and blueschist-facies rocks in northern Syros and south of the village of Kini (Figs. 2a and 3a) are presented below. Most rocks were intensely affected by polyphase deformation. At least three deformation phases took place at high-pressure metamorphic conditions, i.e. at relatively deep crustal levels, whereas additional deformation affected the rocks during and after exhumation into the greenschist-facies field.

3.1. D1 deformation

The earliest recognised structures are preserved as inclusion trails within garnet porphyroblasts in eclogites, but mainly in blueschists (Fig. 4). The mineral assemblage defining this internal fabric includes garnet, rutile, omphacite glaucophane and quartz, indicating eclogite-facies conditions.

D1 structures are represented by internal schistosity (S1), which is usually oblique or even orthogonal to the glaucophane and epidote-bearing matrix foliation (S2) (Fig. 4). The microstructures indicate that garnet growth outlasted the D1 deformation phase, but predated the formation of the external fabric. Few examples show a local curvature of the internal schistosity where the growth of garnet porphyroblasts was possibly accompanied by non-coaxial shearing.

The existence of D1 structures indicates that the deformation associated with HP metamorphism cannot be attributed to a single deformational event. D1 structures record deep

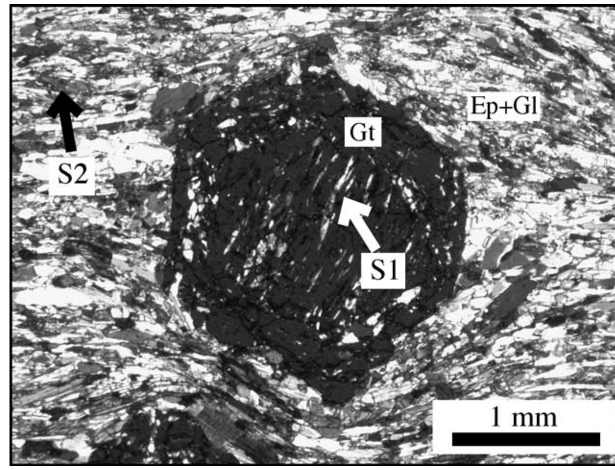

Fig. 4. A photomicrograph showing inclusion trails within garnet porphyroblasts (cross-polarised light). An internal S1 fabric, roughly orothogonal to the external fabric (S2), is recognised in the core of the garnet porphyroblast. The internal fabric is only found in the core of the garnet, whereas no identifiable fabric exists at the rim. Abbreviations: Ep = epidote; Gt = garnet; Gl = glaucophane.

crustal deformation that had occurred prior to the formation of the now-dominant regional high-pressure fabric (D2). We note that a marked obliquity exists between D1 and D2 fabric. It may indicate that a large-scale rigid-body rotation affected the rock sequence between D1 and D2 so as to rotate the internal fabric into vertical, or that strain geometry was modified significantly. We prefer the latter explanation because a rigid-body rotation would be accompanied by significant non-coaxial strain, which is relatively rare in the observed microstructures. Thus, we consider the sub-vertical orientation of S1 an original fabric, which may imply horizontal shortening as the result of upright folding. If so, the transition from D1 to D2 marks a switch from horizontal contraction to vertical thinning.

3.2. D2 deformation

D2 structures are the most prominent features within the high-pressure rocks. These structures are associated with a mineral assemblage of garnet, glaucophane, omphacite, epidote, white mica (phengite or paragonite), quartz and sphene. They include a regional moderately dipping foliation (S2) and glaucophane lineations (L2) that, in northern Syros, trend roughly towards the NW with a mean azimuth of 29°/305° (Fig. 3a and b). The distribution of L2 lineations is clustered on a plane that suggests folding of the lineations on an axis towards 60°/125°. A relatively similar direction (140 ± 10°) has been inferred by Ridley (1982) to explain the variation of glaucophane lineations in a larger scale throughout Syros. Fold axes associated with this folding (F3?) have not been recognised in the study area. The fold direction is normal to the NE-bearing crenulation lineations reported by Ridley (1982) in northern Syros, as well as to the NE direction of tectonic transport considered by Blake

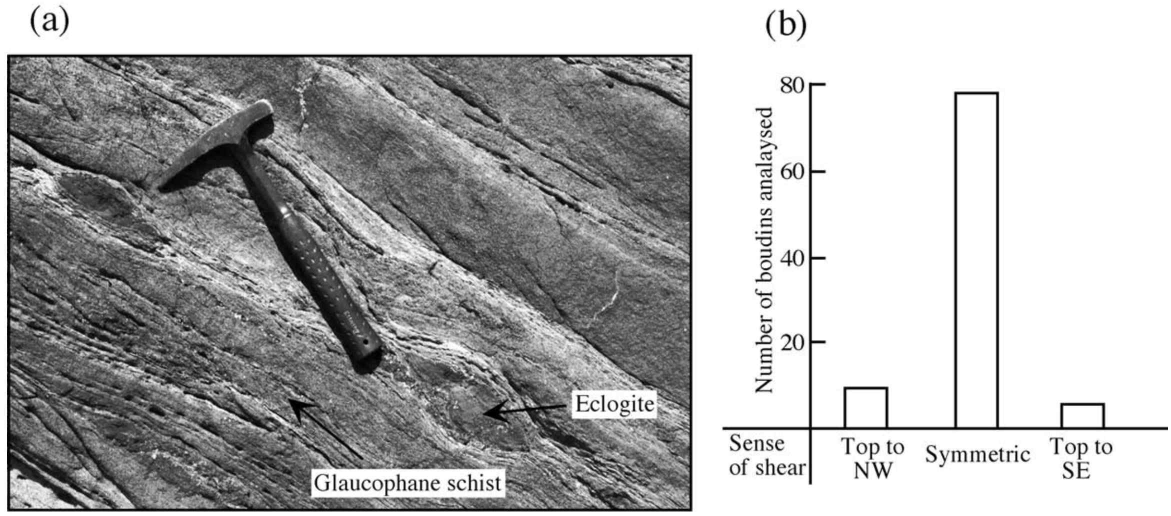

Fig. 5. (a) Eclogitic blocks in ductile tectonites (Kini area). (b) Histogram showing frequency of symmetric and asymmetric blocks within the outcrop shown in (a).

et al. (1981, 1984). According to our results, these features seem to postdate the D2 fabric and are not associated with HP conditions. The effect of the latest NE–SW recumbent to upright folds (Avigad et al., 2001 and references therein) on L2 orientations is not clear. Trotet et al. (2001) have recently reported roughly east bearing glaucophane lineations in Ermoupoli Unit (central-east Syros), which, together with the NW-bearing glaucophane lineations in northern Syros, may suggest a kilometric-scale folding about a SSW-axis that reoriented the bearing of the L2 lineations. This statement, however, should be supported by additional data.

Syn-metamorphic folds (F2) are associated with the D2 fabric. These are tight to isoclinal recumbent folds with axes trending towards the NW (Fig. 3c). As with the glaucophane lineations, a better cluster of the fold axes can be obtained by refolding F2 axes about an axis at ~60°/130°.

D2 deformation is associated with the occurrence of symmetric mesoscopic- to kilometric-scale boudinage structures that suggest horizontal extension and vertical thinning. Mega-scale boudins are symmetrical pinch-and-swell structures that reach a maximum length of 35 m and a thickness of 7 m. They consist of an incompetent marble horizon and a competent omphacite–glaucophane–calc-schist.

In the metabasites south of the village of Kini, numerous ellipsoidal boudins are found within glaucophane-schist tectonites (Fig. 5a). The boudins are predominantly omphacitic in composition and show ductile deformation associated with the D2 fabric. In cross-sections parallel to

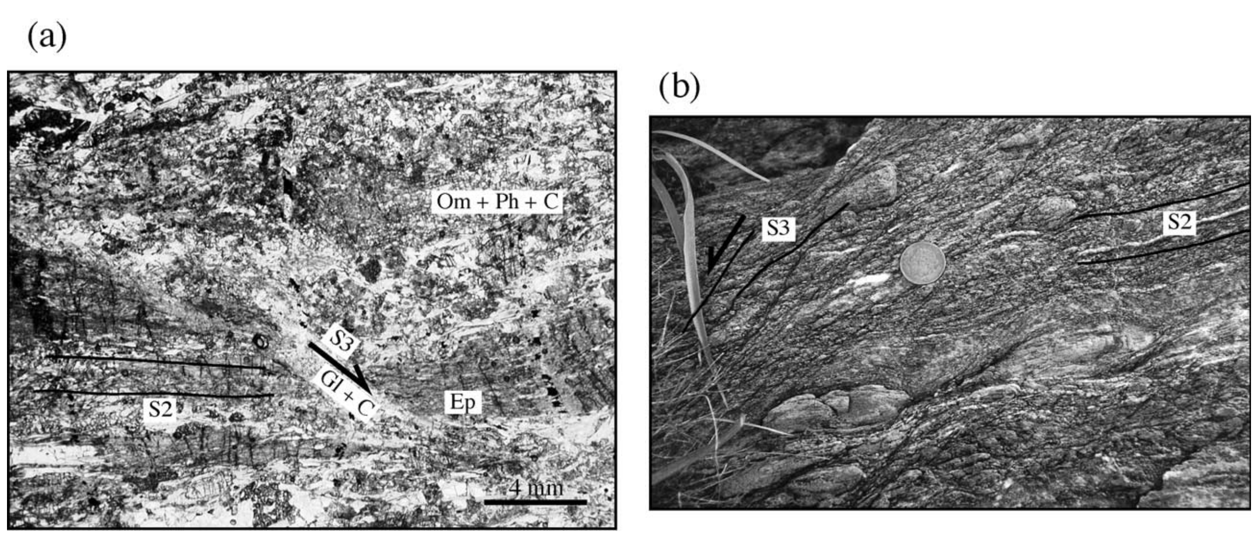

Fig. 6. Structures associated with D3 deformation in northern Syros showing top-to-NW sense of shear. (a) Photomicrograph of recrystallised glaucophane and calcite grains in D3 shear bands that crosscut an older (S2) eclogitic foliation (plane-polarised light). Abbreviations: C = calcite; Ep = epidote; Gl = glaucophane; Om = omphacite; Ph = phengite. (b) Asymmetric boudinage and *S–C* structures.

the mineral lineations, 85% of the boudins had a symmetric appearance, whereas only 15% showed an asymmetry towards the NW or the SE (Fig. 5b).

Pressure-shadows of recrystallised HP minerals (glaucophane, phengite, paragonite and quartz) are common microstructures in the D2 fabric. The structures are usually symmetric, and rarely exhibit a weak asymmetry with uncertain sense of shear.

In short, most of the structures associated with D2 fabrics are oblate and symmetric structures. It is therefore likely that coaxial strain of the bulk of the section in northern Syros and in Kini played a major role during D2 deformation.

3.3. D3 deformation

This deformation phase is superimposed on the earlier D2 fabrics. The deformation is associated with the mineral assemblage of glaucophane, albite, quartz, calcite and sphene. Glaucophane-bearing shear bands (C' planes) are locally well developed in northern Syros and show a weak asymmetry towards the NW (Fig. 6). D3 fabrics are also related to asymmetric boudinage structures found within the dominant omphacite and glaucophane-bearing fabric (S2) (Fig. 6b). Kinematic indicators used for determination of the shear direction are S–C fabric relations, asymmetric boudinage structures and the displacement of grains along shear bands. Based on these relationships, we conclude that D3 structures postdated the main eclogite- and blueschist-facies fabric. It is suggested that D3 structures were formed at the onset of decompression and cooling of the HP sequence, although the possibility that glaucophane grains have been reoriented by later (greenschist-facies) retrograde shear bands cannot be excluded. D3 structures, however, seem to be essentially different from greenschist-facies mylonites (D4) because their shear direction is orthogonal to the top-to-NE shearing associated with D4 structures.

3.4. D4 deformation

D4 deformation is associated with a mineral assemblage of phengite, albite, chlorite, calcite, ankerite and quartz. This deformation took place when the HP sequence decompressed to shallow crustal conditions. Most structures are characterised by asymmetric kinematic criteria (e.g. asymmetric pressure shadows and S–C structures) with top-to-NE sense of shear (Fig. 7).

D4 structures are prominent on a regional scale, especially in areas throughout the Cyclades that underwent a penetrative greenschist-facies overprint. However, in the study areas greenschist-facies assemblages are not common and evidence of D4 structures is relatively rare.

4. Additional evidence from Sifnos

Complementary structural evidence is provided from the

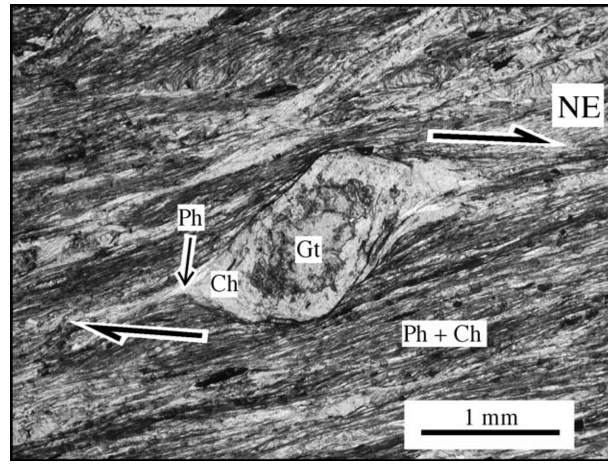

Fig. 7. Photomicrograph showing an asymmetric pressure shadows and S–C structures with top-to-NE sense of shear. The presence of chlorite in the rim of the garnet porphyroblast and in the schistose matrix is indicative for greenschist-facies conditions. Abbreviations: Ch = chlorite; Gt = garnet; Ph = phengite.

island of Sifnos, where HP rocks with similar metamorphic and structural evolution are exposed (Avigad et al., 1992; Avigad, 1993). The following observations were taken from well-preserved eclogite- and blueschist-facies rocks in a coastal cliff overlooking Vroulidia Bay in the northern part of the island (Fig. 2c).

The island of Sifnos, in the western part of the Cyclades (Fig. 1), is entirely made of rocks of the Cycladic Blueschist Unit. The stratigraphic sequence includes four main lithological sub-units, which are, from bottom to top, the Greenschist Unit (originally an eclogite-facies sequence), the Main Marble Unit, the Blueschist–Eclogite Unit and the Upper Marble Unit (Fig. 2c) (Davis, 1966; Okrusch et al., 1978). The high-pressure rocks in Vroulidia Bay consist of blueschists, eclogites and jadeite gneisses that belong to the blueschist–eclogite unit, which form a succession of interlayering metasedimentary rocks with acid and basic metavolcanics. Pressure–temperature (PT) conditions have been estimated by Matthews and Schliestedt (1984), Evans (1986), Schliestedt (1986) and Schliestedt and Matthews (1987) as 440–500 °C at pressures of 14–15 kbar.

The major fabric on northern Sifnos contains a shallow-dipping regional foliation made of eclogite- and blueschist-facies minerals (S2). Our observations concentrated on boudinage structures and deformed conglomerate pebbles from this section with the aim of defining whether these structures can reveal the strain history.

Boudinage structures of eclogitic boudins in metasedimentary matrix occur in an outcrop northwest of Vroulidia Bay. In a section parallel to the mineral lineations, the shapes of the boudins are nearly rectangular and their thickness varies from 10 to 15 cm. The foliation surfaces of the matrix rock are slightly folded towards the neck of the boudin. Recrystallised glaucophane grains were found in the necks, indicating deformation during HP conditions,

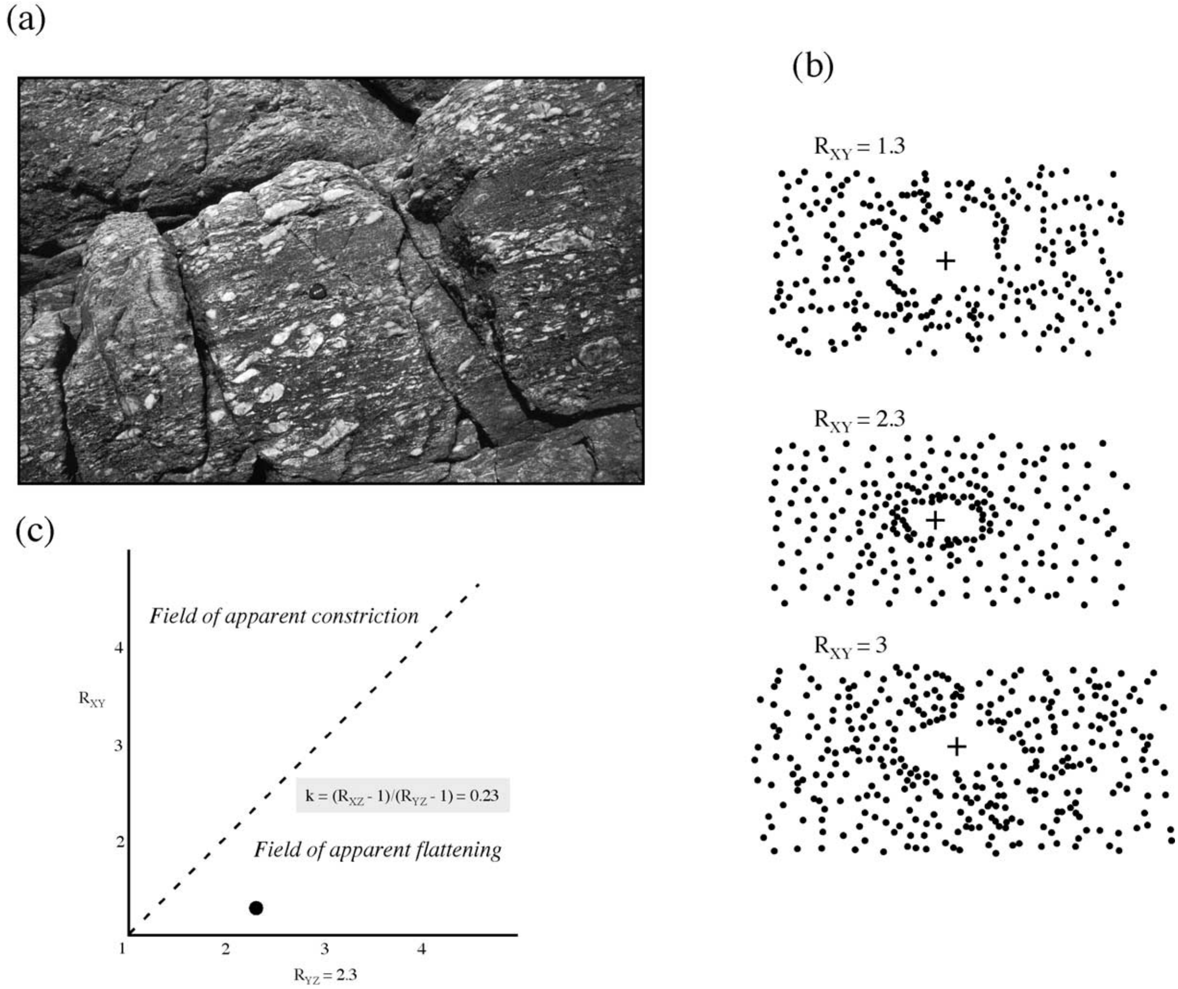

Fig. 8. (a) Photograph showing a deformed calcite pebbles in a mica-schist matrix in Vroulidia Bay (Sifnos). (b) Fry diagrams showing strain ellipses of three orthogonal orientations in deformed conglomerates. (c) Calculated values of principal strain planes plotted on a Flinn diagram. The corresponding *K* value is within the field of apparent flattening.

possibly during D2 deformation. As in the HP rocks on Syros, this deformation suggests a vertical thinning.

The relative dimensions of the local strain ellipsoid were evaluated by examining a unique sequence of deformed conglomerates in Vroulidia Bay (Fig. 8). The conglomerates, consisting of calcite pebbles, are embedded within a HP mica-schist. Plots of strain ellipses in three perpendicular orientations were obtained by the use of the Fry method (Fry, 1979) (Fig. 8b). The longest dimension of the strain ellipsoid indicates 300% of horizontal extension. The principal plane strain (Ramsay and Huber, 1983) plotted on a Flinn diagram (Fig. 8c), indicating a *K* value of 0.23. The corresponding *K* value is within the field of apparent flattening where the strain ellipsoid is oblate.

5. Pressure–temperature constraints

The metamorphic conditions during the deformational history have been constrained using several geothermobarometric methods and by comparison with published petrologic data. The accuracy of these constraints is limited, but they enable us to delineate a schematic pressure–temperature–deformation (PTd) path presented in Fig. 9.

Metamorphic conditions during D1 were estimated using the jadeite content in omphacite inclusions and by the garnet–clinopyroxene geothermometer. Garnet hosts and their associated clinopyroxene inclusions were analysed in a JEOL JXA-8600 electron microprobe (Table 1). Based on the jadeite content of omphacite inclusions ($\sim Jd_{0.50}$; Table 1), a minimum pressure of 11 kbar has been determined (Holland, 1980). Pressures of 13 kbar have been assumed to calculate temperatures using the garnet–clinopyroxene geothermometer (Råheim and Green, 1974; Ellis and Green, 1979; Krogh, 1988). These temperatures are estimated as 450 ± 40 °C on Syros and 470 ± 30 °C on Sifnos.

Constraints on the pressure–temperature conditions during D2 deformation are based on published geothermobarometry associated with HP assemblages on Syros and Sifnos (Dixon, 1976; Matthews and Schliestedt, 1984;

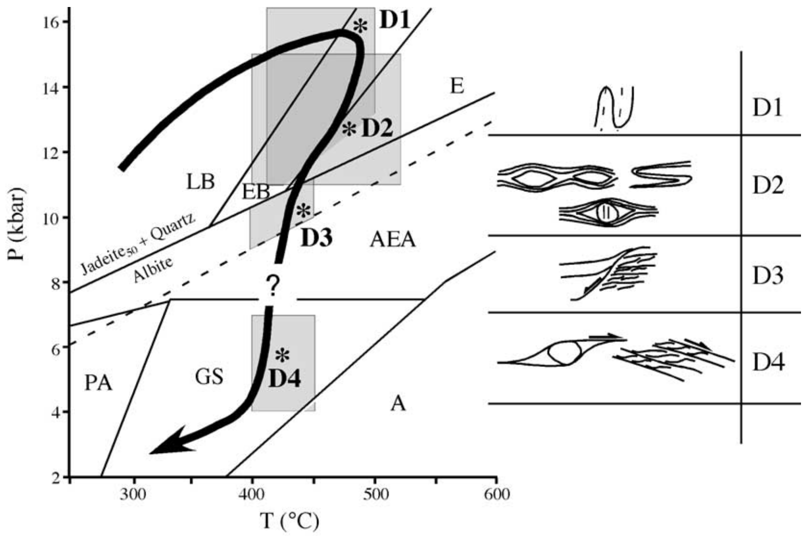

Fig. 9. Schematic PTd diagram and sketches of the structures developed during the burial and exhumation of the HP/LT rocks in the Cycladic massif. Estimated metamorphic conditions during the deformation phases (D1 to D4) are shown in the shaded boxes. Isograds of metamorphic facies are after Evans (1990) for the equilibrium of sodic amphibole with a glaucophane composition. Dashed curve indicates the lower stability field of crossite-rich glaucophane (Evans, 1990). Abbreviations: A = amphibolite facies; AEA = albite–epidote–amphibolite facies; E = eclogite facies; EBS = epidote–blueschist facies; GS = greenschist facies; LBS = lawsonite–blueschist facies; PA = pumpellite–actinolite facies.

Table 1
Result of representative microprobe analyses

Mineral	Omphacite				Garnet		
Sample	GR-1131 Syros	GR-1104 Syros	GR-2214 Sifnos		GR-1131 Syros	GR-1104 Syros	GR-2214 Sifnos
SiO_2	55.66	57.81	56.43		37.68	38.76	38.36
TiO_2	0.00	0.14	0.00		0.00	0.00	0.00
Al_2O_3	10.86	10.83	8.18		20.53	20.24	21.04
FeO	3.81	4.01	4.88		27.43	31.71	29.90
Fe_2O_3	4.82	5.81	3.77		0.00	0.00	0.00
Cr_2O_3	0.00	0.00	0.16		0.00	0.00	0.00
MnO	0.29	0.14	0.00		2.10	1.25	0.94
CaO	10.38	8.48	13.03		9.97	6.97	8.64
MgO	5.47	4.80	7.38		1.31	1.69	1.90
Na_2O	8.49	8.86	6.45		0.04	0.00	0.10
K_2O	0.00	0.00	0.07		0.02	0.00	0.01
Total	99.78	100.88	100.35		99.08	100.62	100.89
Cations							
Si	2.001	2.065	2.039		3.035	3.095	3.031
Al^{IV}	0.000	0.000	0.000		0.000	0.000	0.000
Al^{VI}	0.460	0.456	0.348		1.949	1.905	1.959
Fe^{3+}	0.132	0.158	0.104		0.000	0.000	0.000
Cr	0.000	0.000	0.005		0.000	0.000	0.000
Ti	0.000	0.004	0.000		0.000	0.000	0.000
Fe^{2+}	0.115	0.120	0.148		1.847	2.118	1.976
Mn	0.009	0.004	0.000		0.143	0.085	0.063
Mg	0.293	0.256	0.398		0.157	0.201	0.224
Na	0.592	0.614	0.452		0.000	0.000	0.000
Ca	0.400	0.325	0.504		0.860	0.596	0.731
Sum	4.000	3.996	3.992		7.992	8.000	7.984
Jadeite	46.2	47.3	35.7	Grossular	28.6	19.9	24.4
Acmite	13.2	16.4	10.6	Spessartine	4.8	2.8	2.1
Augite	40.6	36.3	53.7	Almandine	61.4	70.6	66.0
				Pyrope	5.2	6.7	7.5
a_{jd}	0.46	0.46	0.35				

Schliestedt, 1986; Schliestedt and Matthews, 1987; Avigad et al., 1992). In these studies, minerals used for PT determinations have been sampled from rocks that were pervasively affected by the dominant HP fabric. Therefore, the estimated pressures and temperatures seem to indicate the metamorphic conditions during D2 deformation. These studies show that pressures of 11–15 kbar and temperatures of 400–520 °C prevailed during D2 deformation.

The occurrence of blue amphiboles in D3 shear zones was used to determine the minimum pressures during D3 deformation. These are mostly crossite-rich glaucophane grains that indicate pressures of more than 8 kbar (Evans, 1990) (Fig. 9). The absence of clinopyroxene in D3 assemblages suggests that maximum pressures did not exceed the stable equilibrium curve of Jd + Q = Ab. The accuracy of this estimation, however, is limited because the whole-rock chemistry might have changed during the deformation history, affecting the stability field used to confine the conditions during D3 deformation. Avigad et al. (1992) have estimated pressures of 8–10 kbar for albite–blueschists in Sifnos that exhibited a rather similar mineral assemblage as in the D3 structures. It is therefore possible that these conditions are also appropriate for the D3 deformation phase. We have assumed temperatures of 400–450 °C for this assemblage, but no reliable geothermometer was found. D4 mineral assemblages are scarce in the rock bodies studied and the PT conditions are weakly constrained. However, the presence of retrograde minerals, such as chlorite, albite and ankerite in association with D4 microstructures indicates greenschist-facies conditions during this event. Conditions during the greenschist-facies overprint have been estimated regionally as 4–7 kbar and 400–450 °C (Matthews and Schliestedt, 1984; Avigad et al., 1992).

6. Discussion and conclusions

Results of the present study show that structures associated with a high-pressure mineral growth on Syros and Sifnos are generally symmetric and consistent with an oblate finite-strain ellipsoid. We suggest that deep crustal deformation at eclogite- and blueschist-facies conditions did not include a significant component of non-coaxial strain. This is supported by the scarcity of shear-sense indicators within the well-preserved high-pressure rocks, and by the abundance of symmetric structures on sections cut parallel to the mineral lineations. We do not preclude the possibility that non-coaxial strain affected rocks outside the sequence studied. A bulk coaxial vertical shortening is consistent with the dominant fabric of the HP sections preserved on Syros and Sifnos. Vandenberg and Lister (1996) have drawn a similar conclusion based on the absence of asymmetric kinematic indicators in the HP fabric on Ios. It is therefore possible that the vertical shortening inferred from the flat and symmetric schistosity fabrics (in D2 structures) controlled crustal thinning at deep crustal levels during early stages in the exhumation of the high-pressure rock section. The age of this fabric is not well constrained, but it may be older than the Late Eocene as indicated by most radiometric ages of HP minerals in the central Aegean (e.g. Altherr et al., 1979; Andriessen et al., 1979; Maluski et al., 1987; Wijbrans and McDougall, 1988; Bröcker and Enders, 1999). If so, the vertical ductile thinning inferred from the nearly flat orientation of the dominant HP/LT foliation was formed prior to overthrusting of the Cycladic Blueschist Unit onto the Almyropotamos window (Shaked et al., 2000). In that case, this fabric should be classified as syn-orogenic.

The deep crustal fabric differs significantly from shallow-level extensional structures that have been observed close to detachment faults throughout the Cyclades (e.g. Urai et al., 1990; Gautier et al., 1993; Vandenberg and Lister, 1996; Forster and Lister, 1999a; Jolivet and Patriat, 1999). These structures are dominated by non-coaxial strain and usually indicate top-to-NE sense of shear. However, it is important to emphasise that coaxial strain that shaped the deep crust predated non-coaxial strain at shallower levels. The coaxial deep ductile structures in the HP sequence of the Cyclades formed during the Eocene or earlier, whereas the extensional shear fabrics that are close to the detachments probably formed during or after the greenschist-facies overprint, i.e. in the Oligocene–Miocene (Altherr et al., 1982; Bröcker et al., 1993). Based on our observations, we cannot conclude that coaxial vertical thinning in deep crustal levels occurred contemporaneously with upper crustal extension accommodated by non-coaxial shearing. We stress, however, that the combination of upper crustal non-coaxial shearing with deep crustal coaxial vertical thinning is a plausible mechanism for post-orogenic extension (e.g. Andersen and Jamtveit, 1990).

An important observation of this study is the nearly orthogonal sense of shear of D3 and D4 structures. Glaucophane-bearing D3 shear structures, which were formed at a considerable depth, trend towards the NW, whereas, the upper crustal D4 structures are characterised by shearing towards the NE. This kinematic discontinuity indicates a temporal and spatial strain distribution, which seems to contradict the existence of crustal-scale extensional detachments (e.g. Gautier, 2000). Our observations suggest that the role of non-coaxial strain in deep crustal levels was minor, and that post-orogenic extensional detachments did not penetrate the whole crust.

Inclusion trails preserved in garnet porphyroblasts provide unique evidence on an earlier deformation phase whose structural traces are now almost completely erased. The inclusion trails are highly oblique and even orthogonal to the dominant shallow-dipping foliation. We suggest that this stage in the history of crustal thickening involved horizontal shortening and possibly upright folds close to the orogenic roots. A sequence of phases of syn- and post-orogenic vertical thinning followed, and culminated with the formation of the Aegean back-arc basin and the exposure of the Cycladic blueschists and eclogites.

Acknowledgements

Andor Lips and John C. Schumacher are greatly acknowledged for providing constructive reviews of the manuscript. Thanks are due to Z. Garfunkel for discussions and advice, M. Pavlidis for grammatical assistance and M. Krabbendam for comments on an earlier version of the manuscript. We acknowledge funding from the United States–Israel Binational Science Foundation (BSF).

References

Altherr, R., Schliestedt, M., Okrusch, M., Seidel, E., Kreuzer, H., Harre, W., Lenz, H., Wendt, I., Wagner, G.A., 1979. Geochronology of high-pressure rocks on Sifnos (Cyclades, Greece). Contributions to Mineralogy and Petrology 70, 245–255.

Altherr, R., Kreuzer, H., Wendt, I., Lenz, H., Wagner, G.A., Keller, J., Harre, W., Höhndorf, A., 1982. A Late Oligocene/Early Miocene high temperature belt in the Attic–Cycladic crystalline complex (SE Pelagonian, Greece). Geologisches Jahrbuch E23, 97–164.

Altherr, R., Kreuzer, H., Lenz, H., Wendt, I., Harre, W., Dürr, S., 1994. Further evidence for a Late Cretaceous low-pressure/high-temperature terrane in the Cyclades, Greece. Chemie der Erde 54, 319–328.

Andersen, T.B., Jamtveit, B., 1990. Uplift of deep crust during orogenic extensional collapse: a model based on field studies in the Sogn–Sunnfjord region of western Norway. Tectonics 9, 1097–1111.

Andersen, T.B., Osmundsen, P.T., Jolivet, L., 1994. Deep crustal fabrics and a model for the extensional collapse of the southwest Norwegian Caledonides. Journal of Structural Geology 16, 1191–1203.

Andriessen, P.A.M., Boelrijk, N.A.I.M., Hebeda, E.H., Priem, H.N.A., Verdurmen, E.A.T., Verschure, R.H., 1979. Dating the events of metamorphism and granitic magmatism in the Alpine orogen of Naxos (Cyclades, Greece). Contributions to Mineralogy and Petrology 69, 215–225.

Avigad, D., 1993. Tectonic juxtaposition of blueschists and greenschists in Sifnos Island (Aegean Sea)—implications for the Cycladic blueschist belt. Journal of Structural Geology 15, 1459–1469.

Avigad, D., Garfunkel, Z., 1989. Low-angle faults above and below a blueschist belt—Tinos Island, Cyclades, Greece. Terra Nova 1, 182–187.

Avigad, D., Garfunkel, Z., 1991. Uplift and exhumation of high-pressure metamorphic terrains: the example of the Cycladic blueschist belt (Aegean Sea). Tectonophysics 188, 357–372.

Avigad, D., Garfunkel, Z., Jolivet, L., Azañón, J.M., 1997. Back-arc extension and denudation of Mediterranean eclogites. Tectonics 16, 924–941.

Avigad, D., Baer, G., Heimann, A., 1998. Block rotations and continental extension in the central Aegean Sea: palaeomagnetic and structural evidence from Tinos and Mykonos (Cyclades, Greece). Earth and Planetary Science Letters 157, 23–40.

Avigad, D., Ziv, A., Garfunkel, Z., 2001. Ductile and brittle shortening, extension-parallel folds and maintenance of crustal thickness in the central Aegean (Cyclades, Greece). Tectonics 20, 277–287.

Avigad, D., Matthews, A., Evans, B.W., Garfunkel, Z., 1992. Cooling during the exhumation of a blueschist terrane: Sifnos (Cyclades), Greece. European Journal of Mineralogy 4, 619–634.

Azañón, J.M., García-Dueñas, V., Goffé, B., 1998. Exhumation of high-pressure metapelites and coeval crustal extension in the Alpujarride complex (Betic Cordillera). Tectonophysics 285, 231–252.

Balanyá, J.C., García-Dueñas, V., Azañón, J.M., Sánchez-Gómez, M., 1997. Alternating contractional and extensional events in the Alpujarride nappes of the Alboran Domain (Betic, Gibraltar Arc). Tectonics 16, 226–238.

Blake, M.C.J., Bonneau, M., Geyssant, J., Kienast, J.R., Lepvrier, C., Maluski, H., Papanikolaou, D., 1981. A geologic reconnaissance of the Cycladic blueschist belt, Greece. Geological Society of America Bulletin 92, 247–254.

Blake, M.C.J., Bonneau, M., Geyssant, J., Kienast, J.R., Lepvrier, C., Maluski, H., Papanikolaou, D., 1984. 'A geologic reconnaissance of the Cycladic blueschist belt, Greece'. Reply. Geological Society of America Bulletin 95, 119–121.

Bonneau, M., 1984. Correlation of the Hellenide nappes in the south-east Aegean and their tectonic reconstruction. In: Dixon, J.E., Robertson, A.H.F. (Eds.), The Geological Evolution of the Eastern Mediterranean 17. Geological Society, London, Special Publications, pp. 517–527.

Bonneau, M., Blake, M.C.J., Geyssant, J., Kienast, J.R., Lepvrier, C., Maluski, H., Papanikolaou, D., 1980a. Sur la signification des séries métamorphiques (schistes bleus) des Cyclades (Hellénides, Grèce). L'example de l'île de Syros. Comptes Rendus Hebdomadaires des Seances de l'Academie des Sciences D290, 1463–1466.

Bonneau, M., Geyssant, J., Kienast, J.R., Lepvrier, C., Maluski, H., 1980b. Tectonique et métamorphisme haute pression d'âge éocène dans les Hellénides: examples de l'Île de Syros (Cyclades). Comptes Rendus Hebdomadaires des Seances de l'Academie des Sciences D291, 171–174.

Bröcker, M., Franz, L., 1998. Rb–Sr isotope studies on Tinos island (Cyclades, Greece): additional time constraints for metamorphism, extent of infiltration-controlled overprinting and deformational activity. Geological Magazine 135, 369–382.

Bröcker, M., Enders, M., 1999. U–Pb zircon geochronology of unusual eclogite-facies rocks from Syros and Tinos (Cyclades, Greece). Geological Magazine 136, 111–118.

Bröcker, M., Kreuzer, H., Matthews, A., Okrusch, M., 1993. $^{40}Ar/^{39}Ar$ and oxygen isotope studies of polymetamorphism from Tinos island, Cycladic blueschist belt, Greece. Journal of Metamorphic Geology 11, 223–240.

Buick, I.S., 1991. The late Alpine evolution of an extensional shear zone, Naxos, Greece. Journal of the Geological Society of London 148, 93–103.

Davis, E., 1966. Der geologische Bau der Insel Siphnos. Geol. Geophys, Res. Athens 10, 161–220.

Dewey, J.F., 1988. Extensional collapse of orogens. Tectonics 7, 1123–1139.

Dixon, J.E., 1976. Glaucophane schists of Syros, Greece. Bulletin de la Societe Géologique de France 7, 280.

Dixon, J.E., Ridley, J., 1987. Syros. In: Helgeson, H.C. (Ed.). Chemical Transport in Metasomatic Processes. Reidel Publishing Company, Dordrecht, pp. 489–501.

Dürr, S., Altherr, R., Keller, J., Okrusch, M., Seidel, E., 1978. The median Aegean crystalline belt: stratigraphy, structure, metamorphism, magmatism. In: Cloos, H., Roeder, D., Schmidt, K. (Eds.). Alps, Appenines, Hellenides 38. I.U.G.S. Rep, Stuttgart, pp. 455–477.

Ellis, D.J., Green, D.H., 1979. An experimental study of the effect of Ca upon garnet–clinopyroxene Fe–Mg exchange equilibria. Contributions to Mineralogy and Petrology 71, 13–22.

Evans, B.W., 1986. Reactions among sodic, calcic, and ferromagnesian amphiboles, sodic pyroxene, and deerite in high-pressure metamorphesed ironstone, Siphnos, Greece. American Mineralogist 71, 1118–1125.

Evans, B.W., 1990. Phase relations of epidote–blueschist. Lithos 25, 3–23.

Faure, M., Bonneau, M., Pons, J., 1991. Ductile deformation and syntectonic granite emplacement during the late Miocene extension of the Aegea (Greece). Bulletin de la Societe Geologique de France, 5, 3–11.

Forster, M.A., Lister, G.S., 1999a. Detachment faults in the Aegean core complex of Ios, Cyclades, Greece. In: Ring, U., Brandon, M.T., Lister, G.S., Willet, S.D. (Eds.), Exhumation Processes: Normal Faulting,

Ductile Flow and Erosion 154. Geological Society, London, Special Publications, pp. 305–323.
Forster, M.A., Lister, G.S., 1999b. Separate episodes of eclogite and blueschist facies metamorphism in the Aegean metamorphic core complex of Ios, Cyclades, Greece. In: Mac Niocaill, C., Ryan, P.D. (Eds.), Continental Tectonics 164. Geological Society, London, Special Publications, pp. 157–177.
Fry, N., 1979. Random point distributions and strain measurment in rocks. Tectonophysics 60, 89–105.
Gautier, P., 2000. Comments on "Back-arc extension and denudation of Mediterranean eclogites" by Dov Avigad, Zvi Garfunkel, Laurent Jolivet and José M. Azañón. Tectonics 19, 406–409.
Gautier, P., Brun, J.P., 1994. Crustal-scale geometry and kinematics of late-orogenic extension in the central Aegean (Cyclades and Evvia Island). Tectonophysics 238, 399–424.
Gautier, P., Brun, J.P., Jolivet, L., 1993. Structure and kinematics of Upper Cenozoic extensional detachment on Naxos and Paros (Cyclades islands, Greece). Tectonics 12, 1180–1194.
Hecht, J., 1984. Geological map of Greece 1:50,000, Syros island. Ins. Geol. Mineral. Exploration, Athens.
Holland, T.J.B., 1980. The reaction albite = jadeite + quartz determined experimentally in the range 600–1200 °C. American Mineralogist 65, 129–134.
Jolivet, L., Patriat, M., 1999. Ductile extension and the formation of the Aegean Sea. In: Durand, B., Jolivet, L., Horvàth, F., Séranne, M. (Eds.), The Mediterranean Basins: Tertiary Extension within the Alpine Orogen 156. Geological Society, London, Special Publications, pp. 427–456.
Jolivet, L., Dobois, R., Fournier, M., Goffé, B., Michard, A., Jourdan, C., 1990. Ductile extension in Corsica. Geology 18, 1007–1010.
Jolivet, L., Goffé, B., Bousquet, R., Oberhänsli, R., Michard, A., 1998. Detachments in high-pressure mountain belts, Tethyan examples. Earth and Planetary Science Letters 160, 31–47.
Katsikatsos, G., Migiros, G., Triantaphyllis, M., Mettos, A., 1986. Geological structure of internal Hellenides (E. Thessaly–SW. Macedonia, Euboea–Attica–Northern Cyclades islands and Lesvos). IGME Geological and Geophysical Research Special Issue, 191–212.
Keay, S., 1998. The geological evolution of the Cyclades, Greece: constraints from SHRIMP U–Pb geochronology. Ph.D. thesis, Australian National University.
Krogh, E.J., 1988. The garnet clinopyroxene Fe–Mg geothermometer—a reinterpretation of existing experimental data. Contributions to Mineralogy and Petrology 99, 44–48.
Le Pichon, X., Angelier, J., 1979. The Hellenic arc and trench system: a key to the Neotectonic evolution of the eastern Mediterranean area. Tectonophysics 60, 1–42.
Lee, J., Lister, G.S., 1992. Late Miocene ductile extension and detachment faulting, Mykonos, Greece. Geology 20, 121–124.
Lister, G.S., Davis, G.A., 1989. The origin of metamorphic core complexes and detachment faults formed during Tertiary continental extension in the northern Colorado River region, USA. Journal of Structural Geology 11, 65–94.
Lister, G.S., Raouzaios, A., 1996. The tectonic significance of porphyroblastic blueschist facies overprint during Alpine orogenesis: Sifnos, Aegean Sea, Greece. Journal of Structural Geology 18, 1417–1435.
Lister, G.S., Banga, G., Feenstra, A., 1984. Metamorphic core complexes of the Cordilleran type in the Cyclades, Aegean Sea. Geology 12, 221–225.
Lister, G.S., Forster, M.A., Rawling, T., 2001. Episodicity during orogenesis. In: Miller, J.A., Holdsworth, R.E., Buick, I.S., Hand, M. (Eds.), Continental Reactivation and Reworking 184, Geological Society, London, Special Publications pp. 89–113.
Maluski, H., Bonneau, M., Kienast, J.R., 1987. Dating the metamorphic events in the Cycladic area: $^{40}Ar/^{39}Ar$ data from metamorphic rocks of the island of Syros (Greece). Bulletin de la Societe Géologique de France 8, 833–842.
Matthews, A., Schliestedt, M., 1984. Evolution of the blueschist and greenschist facies rocks of Sifnos, Cyclades, Greece. Contributions to Mineralogy and Petrology 88, 150–163.
Okrusch, M., Bröcker, M., 1990. Eclogite associated with high-grade blueschists in the Cyclades archipelago, Greece: a review. European Journal of Mineralogy 2, 451–478.
Okrusch, M., Seidel, E., Davis, E.N., 1978. The assemblage jadeite–quartz in glaucophane rocks of Sifnos (Cyclades, Greece). N. Jb. Miner. Abh. 132, 284–308.
Platt, J.P., 1986. Dynamics of orogenic wedges and the uplift of high-pressure metamorphic rocks. Geological Society of America Bulletin 97, 1037–1053.
Platt, J.P., 1993. Exhumation of high-pressure rocks: a review of concepts and processes. Terra Nova 5, 119–133.
Råheim, A., Green, D.H., 1974. Experimental determination of the temperature and pressure dependence of the Fe–Mg partition coefficient for coexisting garnet and clinopyroxene. Contributions to Mineralogy and Petrology 48, 179–203.
Ramsay, J.G., Huber, M.I., 1983. The Techniques of Modern Structural Geology, Vol. 1, Strain Analysis. Academic Press, London.
Ridley, J., 1982. Arcuate lineation trends in a deep level, ductile thrust belt, Syros, Greece. Tectonophysics 88, 347–360.
Ring, U., Brandon, M.T., Willet, S.D., Lister, G.S., 1999. Exhumation processes. In: Ring, U., Brandon, M.T., Lister, G.S., Willet, S.D. (Eds.), Exhumation Processes: Normal Faulting, Ductile Flow and Erosion 154. Geological Society, London, Special Publication, pp. 1–27.
Schliestedt, M., 1986. Eclogite–blueschist relationships as evidenced by mineral equilibria in the high-pressure metabasic rocks of Sifnos (Cycladic Islands), Greece. Journal of Petrology 27, 1437–1459.
Schliestedt, M., Matthews, A., 1987. Transformation of blueschist to greenschist facies rocks as a consequence of fluid infiltration, Sifnos (Cyclades), Greece. Contributions to Mineralogy and Petrology 97, 237–250.
Shaked, Y., Avigad, D., Garfunkel, Z., 2000. Alpine high-pressure metamorphism at the Almyropotamos window (southern Evia, Greece). Geological Magazine 137, 367–380.
Trotet, F., Jolivet, L., Vidal, O., 2001. Tectono-metamorphic evolution of Syros and Sifnos islands (Cyclades, Greece). Tectonophysics 338, 179–206.
Urai, J.L., Schuiling, R.D., Jansen, J.B.H., 1990. Alpine deformation on Naxos. In: Knipe, R.J., Rutter, E.H. (Eds.), Deformation Mechanisms, Rheology and Tectonics 54. Geological Society, London, Special Publication, pp. 509–522.
Vandenberg, L.C., Lister, G.S., 1996. Structural analysis of basement tectonites from the Aegean metamorphic core complex of Ios, Cyclades, Greece. Journal of Structural Geology 18, 1437–1454.
Wijbrans, J.R., McDougall, I., 1988. Metamorphic evolution of the Attic Cycladic Metamorphic Belt on Naxos (Cyclades, Greece) utilizing $^{40}Ar/^{39}Ar$ age spectrum measurements. Journal of Metamorphic Geology 6, 571–594.